J|A|C|S
ARTICLES
Published on Web 12/12/2003

Attenuating Negative Differential Resistance in an Electroactive Self-Assembled Monolayer-Based Junction

Ronald A. Wassel, Grace M. Credo, Ryan R. Fuierer, Daniel L. Feldheim, and Christopher B. Gorman*

Contribution from the Department of Chemistry, North Carolina State University, Raleigh, North Carolina 27695-8204

Received July 30, 2003; E-mail: chris_gorman@ncsu.edu

Abstract: The negative differential resistance (NDR) peak current observed in redox active self-assembled monolayer-based molecular junctions has been attenuated by controlling the composition of the molecular junction. Two approaches studied here include capping the electroactive ferrocenyl groups with β-cyclodextrin and functionalizing the scanning tunneling microscope tip used to probe the self-assembled monolayer (SAM) with *n*-alkanethiols of different lengths. These are the first examples of systematic modification of the magnitude of the NDR response in a molecule-based system.

Introduction

Metal−molecule−metal junctions exhibiting nonlinear current voltage properties are currently the subject of several research efforts due to their proposed use as elements in molecule-scale electronic components. For example, junctions exhibiting nonlinear current−voltage properties such as negative differential resistance (NDR) are desirable because they could serve as nanoscale analogues of multistate electronic switches.[1−4] NDR behavior in conventional semiconductor-based resonant tunneling diodes (RTDs) has been tuned by modifying the materials, dopant concentration, and the physical configuration of the device.[5−9] However, control of the parameters governing NDR behavior in molecular systems is just beginning to be explored experimentally[3,10−12] and theoretically.[13−17]

Recent scanning probe microscopy studies have described the use of electroactive moieties in molecular junctions to facilitate the appearance of nonlinear current−voltage behavior.[4,14,18−20] Several reports have examined the relationship between NDR and electroactivity in organic[4,18,21] and inorganic systems.[22,23] In semiconductor devices, one mechanism that results in observed NDR is resonant tunneling. A resonant tunneling diode consists of a quantum well separated from two electrical contacts by two tunnel barriers. In semiconductor devices, the quantum well is composed of a narrow layer of material characterized by accessible quantized states (as in the well/barrier system GaAs/AlGaAs).[5] In resonant tunneling, the tunnel barriers control the probability of electrons moving from one electrode to the other through the quantum well. In an analogous molecular device (Figure 1), electroactive molecules appear to serve a similar role via accessible energy levels for electron tunneling. In RTDs, the magnitude of the NDR current peak, directly related to the resonant tunneling probability, is affected by the height and width of the barriers on each side of the well.[6−9] Tunability for conventional RTDs suggests that NDR behavior in molecular-scale systems should also exhibit predictable changes based on tunnel barrier modifications. Several relevant studies suggest that molecule-based tunnel barriers can be constructed in a rational manner.[24−30]

(1) Sze, S. M. *Physics of Semiconductor Devices*, 2nd ed.; John Wiley & Sons: New York, 1981.
(2) Chen, J.; Reed, M. A.; Rawlett, A. M.; Tour, J. M. *Science* **1999**, *286*, 1550−1552.
(3) Selzer, Y.; Salomon, A.; Ghabboun, J.; Cahen, D. *Angew. Chem., Int. Ed.* **2002**, *41*, 827−830.
(4) Gorman, C. B.; Carroll, R. L.; Fuierer, R. R. *Langmuir* **2001**, *17*, 6923−6930.
(5) Sun, J. P.; Haddad, G. I.; Mazumder, P.; Schulman, J. N. *Proc. IEEE* **1998**, *86*, 641−661.
(6) Zhao, P.; Cui, H. L.; Woolard, D.; Jensen, K. L.; Buot, F. A. *J. Appl. Phys.* **2000**, *87*, 1337−1349.
(7) Huang, C. Y.; Morris, J. E.; Su, Y. K.; Kuo, T. H. *Electron. Lett.* **1994**, *30*, 1012−1013.
(8) Zhao, P.; Cui, H. L.; Woolard, D. L.; Jensen, K. L.; Buot, F. A. *IEEE Trans. Electron Devices* **2001**, *48*, 614−627.
(9) Schulman, J. N.; Santos, H. J. D. L.; Chow, D. H. *IEEE Electron Device Lett.* **1996**, *17*, 220−222.
(10) Xue, Y.; Datta, S.; Ratner, M. A. *J. Chem. Phys.* **2001**, *115*, 4292−4299.
(11) Lu, X.; Hipps, K. W. *J. Phys. Chem. B* **1997**, *101*, 5391−5396.
(12) Song, I. K.; Kaba, M. S.; Barteau, M. A. *Langmuir* **2002**, *18*, 2358−2362.
(13) Leonard, F.; Tersoff, J. *Phys. Rev. Lett.* **2000**, *85*, 4767−4770.
(14) Karzazi, Y.; Cornil, J.; Brédas, J. L. *J. Am. Chem. Soc.* **2001**, *123*, 10076−10084.
(15) Paulsson, M.; Stafstrom, S. *Phys. Rev. B* **2001**, *64*, 035416.
(16) Han, J. E.; Crespi, V. H. *Appl. Phys. Lett.* **2001**, *79*, 2829.
(17) Seminario, J. M.; Zacarias, A. G.; Tour, J. M. *J. Phys. Chem. A* **1999**, *103*, 7883−7887.
(18) Tao, N. J. *Phys. Rev. Lett.* **1996**, *76*, 4066−4069.
(19) Hipps, K. W.; Barlow, D. E.; Mazur, U. *J. Phys. Chem. B* **2000**, *104*, 2444−2447.
(20) Scudiero, L.; Barlow, D. E.; Hipps, K. W. *J. Phys. Chem. B* **2000**, *104*, 11899−11905.
(21) Chen, J.; Wang, W.; Reed, M. A.; Rawlett, A. M.; Price, D. W.; Tour, J. M. *Appl. Phys. Lett.* **2000**, *77*, 1224−1226.
(22) Kinne, M.; Barteau, M. A. *Surf. Sci.* **2000**, *447*, 105−111.
(23) Kaba, M. S.; Song, I. K.; Barteau, M. A. *J. Vac. Sci. Technol., A* **1997**, *15*, 1299−1304.
(24) Boulas, C.; Davidovits, J. V.; Rondelez, F.; Vuillaume, D. *Phys. Rev. Lett.* **1996**, *76*, 4797−4800.
(25) Holmlin, E. E.; Haag, R.; Chabinyc, M. L.; Ismagilov, R. F.; Cohen, A. E.; Rampi, M. A.; Terfort, A.; Whitesides, G. M. *J. Am. Chem. Soc.* **2001**, *123*, 5075−5085.
(26) Holmlin, R. E.; Ismagilov, R. F.; Haag, R.; Mujica, V.; Ratner, M. A.; Rampi, M. A.; Whitesides, G. M. *Angew. Chem., Int. Ed.* **2001**, 2316−2320.
(27) Wold, D. J.; Frisbie, C. D. *J. Am. Chem. Soc.* **2000**, *122*, 2970−2971.
(28) Wold, D. J.; Frisbie, C. D. *J. Am. Chem. Soc.* **2001**, *123*, 5549−5556.

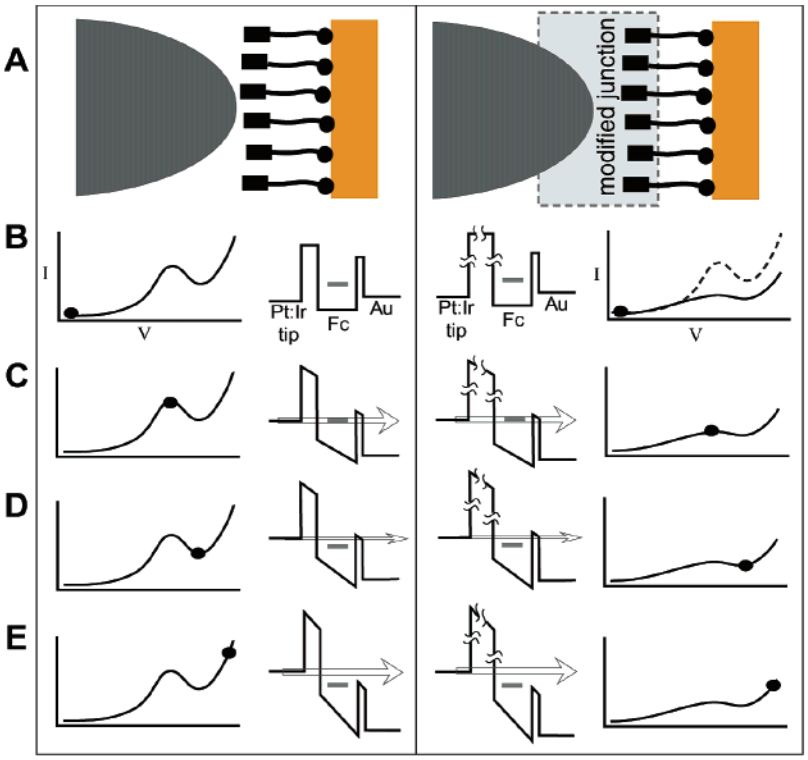

Figure 1. Qualitative model for the attenuation of NDR peak current by modification of the STM tip/ferrocenyl tunnel junction. (A) Schematics of the two junctions and energy level diagrams indicating the two junctions (B) at zero applied bias, (C) in resonance with the molecular orbital (MO) associated with the ferrocenyl headgroups, (D) out of resonance with the MO associated with the ferrocenyl headgroups, and (E) exhibiting an increase in nonresonant current.

In this paper, the results of modulating the tunnel barrier in a molecule-based system are reported. In the first example, the tunnel barrier between a ferrocene-terminated self-assembled monolayer ($FcC_{11}S$-SAM) and a scanning tunneling microscope (STM) tip was modulated by the formation of host−guest complexes consisting of cyclodextrin-ferrocene. The second system consisted of a $FcC_{11}S$-SAM in contact with an STM tip that had been functionalized by *n*-alkanethiols of different lengths. It was hypothesized that the magnitude of the tunneling barrier between the ferrocenyl group and the STM tip could be modulated by these structural modifications to the barrier. These modifications were expected and found to decrease the peak current observed through the junction as the result of increasing the effective barrier.

The proposed mechanism for NDR based on resonant tunneling is illustrated qualitatively in Figure 1.[4] A double tunnel junction was formed by the placement of an electroactive moiety between two metal/molecule junction barriers. The tunnel junction was not likely to be symmetric due to the differences between the alkylthiolate Au−S bond on the substrate side and the gap between the ferrocene headgroup and STM tip.[30,31] The precise shape of the tunneling barriers is unknown, but the increase in tunnel barrier with increasing molecular length is precedented as discussed above. On the left side of Figure 1A, resonant tunneling through a ferrocenyl group is depicted using an unmodified tip. On the right side of Figure 1A, placing another chemical species between the tip and ferrocenyl group is suggested to alter the tunnel barrier between tip and ferrocene (via an increase in the width and/or height of the barrier). Figure 1B depicts negligible resonant tunneling current with zero applied bias on the substrate. With an increase in substrate potential, a maximum in peak current is observed as tunneling occurs through a resonant molecular state (Figure 1C). Whether this is the highest occupied molecular orbital (HOMO)[15] or lowest occupied molecular orbital (LUMO)[32] is unclear but depends on the relative Fermi energies of the metal contacts with respect to the molecule in the junction. In Figure 1D, as the coupling between the tip and a resonant state in the molecule reaches a minimum value, current decreases. Finally, in Figure 1E, as the substrate potential becomes more positive, current continues to increase via other injection processes such as thermionic emission.

Results and Discussion

A. Modulation of the Tunnel Barrier Using Noncovalent Complexation of the Electroactive Group. It was hypothesized that reduction in the electron-transfer rate due to the capping of the ferrocenyl (Fc) groups with β-cyclodextrin (β-CD) would result in a decrease in the magnitude of the observed NDR. Electrochemical studies of Fc-CD complexes in solution have exhibited slowed electron-transfer kinetics following exposure of the Fc to CD as a result of the formation of a 1:1 host−guest inclusion complex.[33−39] In an electrochemical experiment,

(29) Cui, X. D.; Primak, A.; Zarate, X.; Tomfohr, J.; Sankey, O. F.; Moore, A. L.; Moore, T. A.; Gust, D.; Harris, G.; Lindsay, S. M. *Science* **2001**, *294*, 571−574.
(30) Cui, X. D.; Zarate, X.; Tomfohr, J.; Sankey, O. F.; Primak, A.; Moore, A. L.; Moore, T. A.; Gust, D.; Harris, G.; Lindsay, S. M. *Nanotechnology* **2002**, *13*, 5−14.
(31) Collier, C. P.; Jeppesen, J. O.; Luo, Y.; Perkins, J.; Wong, E. W.; Heath, J. R.; Stoddart, J. F. *J. Am. Chem. Soc.* **2001**, *123*, 12632−12641.
(32) Bhatt, J.; Fung, B. M.; Nicholas, K. M. *J. Organomet. Chem.* **1991**, *413*, 263−268.
(33) Ju, H.; Leech, D. *Langmuir* **1998**, *14*, 300−306.

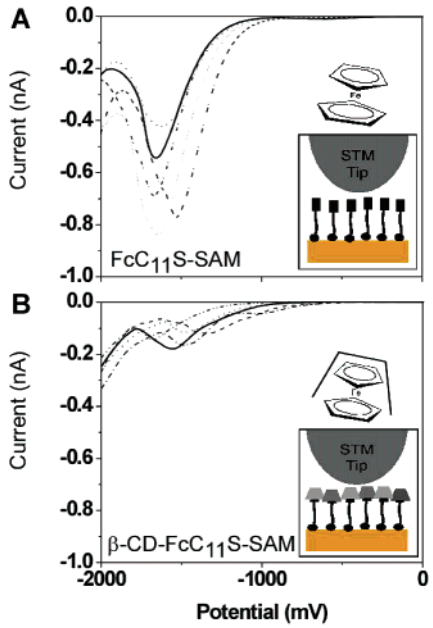

Figure 2. Current−voltage curves of $FcC_{11}S$-SAM before (A) and after (B) exposure to β-CD, as indicated. The insets are schematics of the STM tip-based molecular junctions and are not drawn to scale.

the presence of the cyclodextrin slows the kinetics of electron transfer to the ferrocenyl moiety. Although the cyclodextrin has several effects on the electrochemistry that are not relevant here (e.g., its effect on the diffusion rate of the ferrocene and access of counterions to the oxidized form), a similar complexation was expected to increase the magnitude of the tunnel barrier and result in a decrease in the steady-state current flowing through the ferrocenyl moiety when in a tip−molecule−substrate junction.

After an unmodified $FcC_{11}S$-SAM was scanned and I−V curves exhibiting the same NDR behavior previously reported were measured,[4] this same sample was incubated in an aqueous solution containing β-CD, rinsed, and I−V curves were obtained by STM. Following exposure to the complexation agent, the I−V behavior of the $FcC_{11}S$-SAM exhibited a marked attenuation in peak current as can be observed in Figure 2. Figure 2A shows several representative I−V traces for an unmodified $FcC_{11}S$-SAM as probed by an STM tip. Figure 2B shows analogous I−V traces for a $FcC_{11}S$-SAM that had been incubated in β-cyclodextrin prior to collection of the data. Several traces are shown to indicate the variation observed across a large dataset. However, the peak current was observed to decrease by approximately a factor of 4 as the result of complexation with the β-CD. To rule out nonspecific binding, similar samples were exposed to α-cyclodextrin, a molecule that has an internal cavity that is too small to bind to ferrocene. The type of peak current attenuation observed as the result of complexation with β-cyclodextrin was not observed. Data were also obtained on a dodecanethiolate SAM ($C_{12}S$-SAM), which had no electroactive functionality, to verify that this system did not exhibit NDR response.[4,28,29]

The curves shown in Figure 2 are representative of a larger data set. Sets of 1024 current−voltage traces captured across several regions of each sample were examined. The peak-to-valley ratio (PVR)[2,40] of each curve was tabulated. PVR indicates the ratio of the peak current to the minimum current measured in the region of negative differential resistance. An average PVR of 2.14 ± 1.56 was determined for $FcC_{11}S$-SAMs, which was larger than the average PVR of 1.39 ± 0.48 determined for $FcC_{11}S$-SAMs complexed with β-CD.

Current−distance (I−s) spectroscopy was employed as a complementary method to quantify the change in tunnel barrier upon β-CD complexation. In this experiment, the exponential decrease in current is measured as the tip was retracted vertically from the substrate. This type of analysis was originally employed for the measurement of tunnel barriers in clean, metal/vacuum/metal[41,42] (or semiconductor)[43−46] junctions. This technique then evolved into the study of tunneling through thin water layers.[47,48] Most recently, I−s spectroscopy has been employed in the analysis of metal/molecule/metal junctions.[49,50] In this latter case, the physical significance of the tunnel barrier calculated from these data is more ambiguous.[50] Nevertheless, I−s spectroscopy appears to be a quantitative way to show that the modification of the tunnel junction affects the current−voltage behavior.[51]

To measure the variation in the tunneling barrier, current versus distance measurements were obtained on four types of samples: dodecanethiolate self-assembled monolayers on gold ($C_{12}S$-SAMs), $FcC_{11}S$-SAMs, $FcC_{11}S$-SAMs that had been exposed to β-CD (abbreviated β-CD-$FcC_{11}S$-SAM), and $FcC_{11}S$-SAMs that had been exposed to α-CD (abbreviated α-CD-$FcC_{11}S$-SAM, although this latter molecule is not expected to bind to the $FcC_{11}S$-SAM). The α-CD-$FcC_{11}S$-SAM was employed as a control experiment to rule out modulation of tunneling due to adventitious adsorption onto the SAM. From these data, an apparent tunneling barrier (ϕ) was calculated. This quantity is defined as:

(34) Isnin, R.; Salem, C.; Kaifer, A. E. *J. Org. Chem.* **1991**, *56*, 35−41.
(35) McCormack, S.; Russell, N. R.; Cassidy, J. F. *Electrochim. Acta* **1992**, *37*, 1939−1944.
(36) Suzuki, I.; Chen, Q.; Ueno, A.; Osa, T. *Bull. Chem. Soc. Jpn.* **1993**, *66*, 1472−1481.
(37) Matsue, T.; Evans, D. H.; Osa, T.; Kobayashi, N. *J. Am. Chem. Soc.* **1985**, *107*, 3411−3417.
(38) Szejtli, J. *Chem. Rev.* **1998**, *98*, 1743−1753.
(39) Schönherr, H.; Beulen, M. W. J.; Bugler, J.; Huskens, J.; van Veggel, F.; Reinhoudt, D. N.; Vancso, G. J. *J. Am. Chem. Soc.* **2000**, *122*, 4963−4967.
(40) Borgstrom, M.; Bryilert, T.; Sass, T.; Gustafson, B.; Wernersson, L.-E.; Seifert, W.; Samuelson, L. *Appl. Phys. Lett.* **2001**, *78*, 3232−3234.
(41) Wiesendanger, R. *Scanning Probe Microscopy and Spectroscopy: Methods and Applications*; Cambridge University Press: Cambridge, England; New York, 1994.
(42) Besenbacher, F. *Rep. Prog. Phys.* **1996**, *59*, 1737−1802.
(43) Altfeder, I. B.; Golovchenko, J. A.; Narayanamurti, V. *Phys. Rev. Lett.* **2001**, *8705*, art. no.-056801.
(44) Meepagala, S. C.; Real, F. *Phys. Rev. B* **1994**, *49*, 10761−10763.
(45) Grandidier, B.; Nys, J. P.; Stievenard, D.; de la Broise, X.; Delerue, C.; Lannoo, M. *Appl. Phys. A-Mater. Sci. Process.* **1998**, *66*, S977−S980.
(46) Stievenard, D.; Grandidier, B.; Nys, J. P.; de la Broise, X.; Delerue, C.; Lannoo, M. *Appl. Phys. Lett.* **1998**, *72*, 569−571.
(47) Song, M. B.; Jang, J. M.; Bae, S. E.; Lee, C. W. *Langmuir* **2002**, *18*, 2780−2784.
(48) Hahn, J. R.; Hong, Y. A.; Kang, H. *Appl. Phys. A-Mater. Sci. Process.* **1998**, *66*, S467−S472.
(49) Gittins, D. I.; Bethell, D.; Schiffrin, D. J.; Nichols, R. J. *Nature* **2000**, *408*, 67−69.
(50) Fan, F. R. F.; Yang, J. P.; Cai, L. T.; Price, D. W.; Dirk, S. M.; Kosynkin, D. V.; Yao, Y. X.; Rawlett, A. M.; Tour, J. M.; Bard, A. J. *J. Am. Chem. Soc.* **2002**, *124*, 5550−5560.
(51) Note that this type of measurement, in which the tip is moved relative to the SAM, is not the same as that in which the current through a molecule-based junction is measured for a set of isostructural molecules of differing length. This latter type of experiment calculates a distance dependence of a steady-state current, β, where $i = i_o \exp(-\beta d)$ and d is the length of the molecule.

$$\phi = \left(1/1.025 \frac{\partial \ln i}{\partial S}\right)^2$$

where S is the relative distance of the tip as it was retracted from the sample.[42] The use of this equation in establishing tunneling barriers has been discussed in detail previously.[52,53] Because the initial distance of the tip from the SAM is unknown, the relative interaction of the tip with the SAM is unknown, leading to ambiguity in the physical significance of this quantity. For our purposes, we are only concerned with the comparison of ϕ in the various monolayers studied.

Figure 3 illustrates the range of ϕ values measured across several data sets with different tips and samples. Variation in each type of assembly was observed (similar to that observed in the current−voltage data shown in Figure 2). Reasons for this variation that have been previously proposed include fluctuation in tip−sample geometry, the orientation of the molecules on the surface, and the shape of the tip during the experiment. Nevertheless, trends in the variation of this ϕ value can be obtained. As compared to a C_{12}S-SAM (with an average ϕ, $\phi_{avg} = 1.1 \pm 0.3$, Figure 3A), the average tunneling barrier for FcC_{11}S-SAMs ($\phi_{avg} = 0.31 \pm 0.22$, Figure 3B) is reduced by a factor of approximately 4. Upon complexation, the β-CD-FcC_{11}S-SAM substrate shows an increased average tunnel barrier ($\phi_{avg} = 0.92 \pm 0.67$, Figure 3C). This result was anticipated given the expected increase in barrier required to tunnel through the β-CD. Notably, these data show a wider distribution. This plausibly was due to incomplete encapsulation of every ferrocenyl group by a β-CD. In contrast, little change in the α-CD-FcC_{11}S-SAM data was observed ($\phi_{avg} = 0.39 \pm 0.32$, Figure 3D) as compared to those in Figure 3B, consistent with a noncomplexed FcC_{11}S-SAM. This result ruled out alteration of the tunnel barrier due to nonspecific adsorption or other contamination during the incubation step.

To further support the contention that β-CD complexes with FcC_{11}S-SAM but α-CD does not, PM-IRRAS spectra were obtained on FcC_{11}S-SAM, β-CD-FcC_{11}S-SAM, and FcC_{11}S-SAM that had been incubated with α-CD (indicated as α-CD-FcC_{11}S-SAM). The most diagnostic peak in the FcC_{11}S-SAM was a strong peak at 1107 cm^{-1} which is assigned as a γ(CH) mode on the ferrocenyl moiety based on assignments previously reported by Porter et al.[54] In the α-CD-FcC_{11}S-SAM samples, no differences were observed as compared to the FcC_{11}S-SAM samples. When β-CD-FcC_{11}S-SAM samples were prepared in an identical fashion (e.g., incubation with the cyclodextrin for 24 h followed by rinsing with water and ethanol), the γ(CH) mode on the ferrocenyl moiety shifted to 1085 cm^{-1} and a new mode at 1157 cm^{-1} was observed. This latter band is assigned to C−O stretching in the cyclodextrin. These data are all consistent with surface-bound complexation of β-CD and FcC_{11}S-SAM but a lack of complexation between α-CD and FcC_{11}S-SAM.

B. Modulation of the Tunnel Barrier Using SAMs Attached to the STM Tip. To determine the effect of a systematically increased barrier layer between the tip and the sample, STM tips coated with *n*-alkanethiols of different chain lengths were used to probe Fc-SAM on gold in the configuration shown in the inset of Figure 4. In separate experiments, tips (alternatively Au or Pt:Ir gave similar results) were coated with propanethiol ($CH_3(CH_2)_2SH$ or C3SH), hexanethiol ($CH_3(CH_2)_5$-SH or C6SH), heptanethiol ($CH_3(CH_2)_6SH$ or C7SH), dodecanethiol ($CH_3(CH_2)_{11}SH$ or C12SH), or hexadecanethiol ($CH_3(CH_2)_{15}SH$ or C16SH). The formation of SAMs on the STM tip was expected to occur in a manner similar to that demonstrated in previous work.[55−59]

Current−voltage (I−V) curves were obtained of Fc-SAM using *n*-alkanethiol coated tips and compared to I−V curves obtained using an uncoated tip. When the average response in each data set were compared, a systematic decrease in the average peak current value of the NDR was observed as the chain length of the thiol on the tip was increased.[60] Representative I−V curves illustrating this trend are shown in Figure 4.

Conclusions

The rational attenuation of molecule-based NDR behavior in electroactive, ferrocene-terminated thiolate SAMs at room temperature has been demonstrated. This result has been obtained in two complementary ways: via noncovalent encapsulation of the ferrocenyl groups using β-cyclodextrin, and via coating the tip with *n*-alkylthiolate SAMs of various lengths. The magnitude of the peak tunneling current decreases with increasing tunnel barrier, as has been proposed in conventional resonant tunneling diodes. This tunnel barrier has also been quantitatively probed using current−distance spectroscopy.

From the standpoint of device engineering, functionalization of one contact in an RTD to reduce the peak current is desired in some cases. These include lower power consumption due to lower turn-on voltage and faster switching time, because it would take less time to reach the peak current.[5] Ideally, this is done without losing signal-to-noise ratio. In the case of semiconductor-based RTDs, the quantitative relationship between the tunnel barrier and observed peak current is complex.[7−9] In general, however, an increase in tunnel barrier height or width reduces the steady-state current through the device. These data provide a measure of how tunnel barriers attenuate peak current at the molecular level in a SAM-based system.

Experimental Section

Materials. Dodecane and *n*-alkanethiols ($HS(CH_2)_{n-1}CH_3$ (n = 3, 6, 7, 12, 16) were purchased from Aldrich and were used without further purification. 11-Ferrocenylundecanethiol ($Fc(CH_2)_{11}SH$, abbreviated here as $FcC_{11}SH$) was prepared according to previously published procedures.[61,62] *n*-Alkanethiols were dissolved in anhydrous ethanol (Aaper Alcohol and Chemical Co.) to form 1 mM stock solutions. β-Cyclodextrin (β-CD) was purchased from Fluka, and α-cyclodextrin (α-CD) was purchased from Sigma. Both cyclodextrin molecules were used without further purification. Cyclodextrins were dissolved in

(52) Olesen, L.; Brandbyge, M.; Sorensen, M. R.; Jacobsen, K. W.; Laegsgaard, E.; Stensgaard, I.; Besenbacher, F. *Phys. Rev. Lett.* **1996**, *76*, 1485−1488.
(53) Olesen, L.; Laegsgaard, E.; Stensgaard, I.; Besenbacher, F. *Appl. Phys. A-Mater. Sci. Process.* **1998**, *66*, S157−S160.
(54) Popenoe, D. D.; Deinhammer, R. S.; Porter, M. D. *Langmuir* **1992**, *8*, 2521−2530.
(55) Ohshiro, T.; Ito, T.; Bühlmann, P.; Umezawa, Y. *Anal. Chem.* **2001**, *73*, 878−883.
(56) Go, E. P.; Theuermer, K.; Reutt-Robey, J. E. *J. Phys. Chem. B* **2000**, *104*, 8507−8511.
(57) Jiang, P.; Liu, Z. F.; Wang, Y. C.; Cai, S. M. *Mol. Cryst. Liq. Cryst. Sci. Technol., Sect. A* **2001**, *3337*, 317−320.
(58) Ito, T.; Bühlmann, P.; Umezawa, Y. *Anal. Chem.* **1998**, *70*, 255−259.
(59) Ito, T.; Bühlmann, P.; Umezawa, Y. *Anal. Chem.* **1999**, *71*, 1699−1705.
(60) Wong, E. W.; Collier, C. P.; Behloradsky, M.; Raymo, F. M.; Stoddart, J. F.; Heath, J. R. *J. Am. Chem. Soc.* **2000**, *122*, 5831−5840.
(61) Gorman, C. B.; Miller, R. L.; Chen, K.-Y.; Bishop, A. R.; Haasch, R. T.; Nuzzo, R. G. *Langmuir* **1998**, *14*, 3312−3319.
(62) Uosaki, K.; Sato, Y.; Kita, H. *Langmuir* **1991**, *7*, 1510−1514.

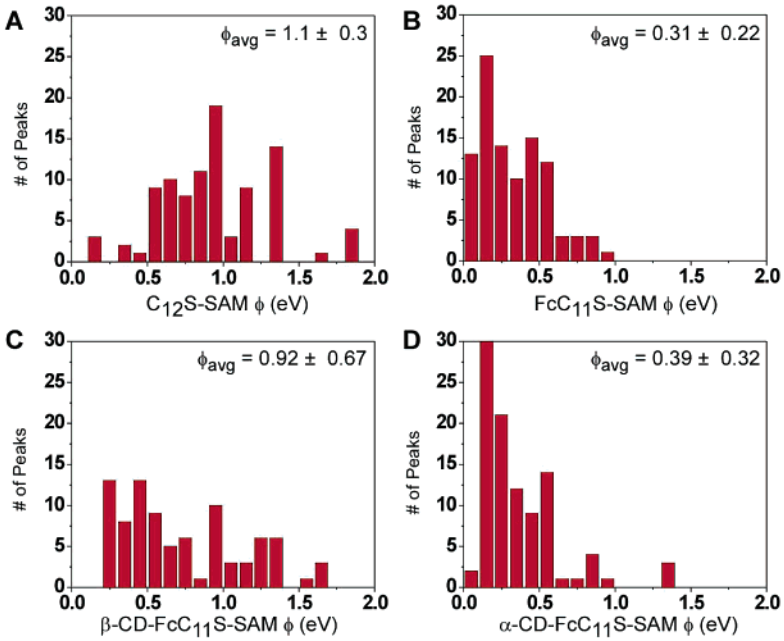

Figure 3. Histograms tabulating the apparent tunnel barriers measured for (A) C_{12}S-SAM, (B) FcC_{11}S-SAM, (C) β-CD-FcC_{11}S-SAM, and (D) α-CD-FcC_{11}S-SAM. Average values ± one standard deviation; ϕ_{avg} are indicated.

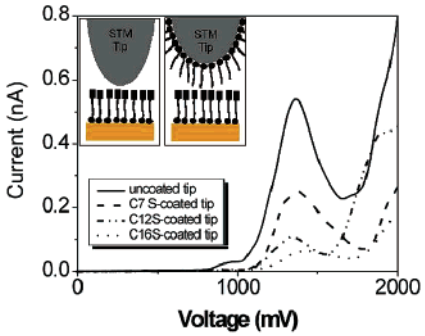

Figure 4. Current−voltage curves of Fc-SAM measured using STM tips coated with *n*-alkylthiolate SAMs, as indicated. The insets are schematics of the STM tip-based molecular junctions before (left) and after (right) coating the STM tip and are not drawn to scale.

deionized water to form 5 mM stock solutions. All solutions were discarded after each use.

SAM Preparation. Sample substrates were flame-annealed Au(111) facets on a gold bead formed at the end of a gold wire (Alfa Aesar, 99.999%). The wire stem was alloyed to a platinum foil (Alfa Aesar) base.[4] Prior to monolayer deposition, the substrates were cleaned in piranha solution (3:1 H_2SO_4:H_2O_2 (30%) by volume). *Caution: Piranha solution is corrosive. In addition, care should be taken to not store piranha solution for extended lengths of time due to the formation of explosive oxides.* Au(111) substrates were incubated in 1 mM ethanol solution of ferrocenyl undecylthiol for at least 24 h at room temperature to form a ferrocenyl-terminated self-assembled monolayer (FcC_{11}S-SAM). After copious rinsing in ethanol and drying in a dinitrogen stream, the sample holder was mounted in a custom Kel-F fluid cell in preparation for scanning in solvent.

Ferrocene-Cyclodextrin Complexation. Au(111) substrates coated with a FcC_{11}S-SAM were incubated in 5 mM aqueous solution of β-CD or α-CD for at least 12 h at room temperature. Samples were rinsed in water and then ethanol and dried in an N_2 stream. Samples were subsequently studied by STM without further delay.

Tip Coating with Thiols. The STM tips used in this work were mechanically cut Pt:Ir (90:10, Alfa Aesar, 0.254 mm diameter) or Au (99.995%, Alfa Aesar, 0.254 mm diameter) wire. Prior to exposure to neat thiol, they were immersed in piranha solution for 30 s, rinsed with water and then absolute ethanol, and dried in an N_2 stream. The tips were then immersed overnight in neat thiol under ambient conditions. Prior to use, the tips were rinsed in absolute ethanol and dried in an N_2 stream.

Scanning Tunneling Microscopy (STM). All current−voltage data were collected on a Digital Instruments (Santa Barbara, CA) Nanoscope E, equipped with a multimode base, an E-scanner, and low-current converter with a picoamp boost stage. All experiments were performed at room temperature under ambient conditions. Current−distance (I−s) measurements were performed using a RHK (Troy, MI) SPM 1000 controller with the same Digital Instruments multimode base, E-scanner, and low-current converter. The sample substrate was placed in a custom-made Kel-F fluid cell and scanned in a low dielectric solvent, such as dodecane or mesitylene. Typical scanning conditions for both types of measurements were a bias voltage of 1 V and a set-point current of 10 pA.

Scanning Tunneling Spectroscopy (I−V Data Collection). Current−voltage curves were collected for these experiments using the CITS (current imaging tunneling spectroscopy) mode in the Digital Instruments scanning software. At least three data sets for each type of experiment were collected. Each set consisted of 1024 curves collected at regularly spaced intervals (32 × 32 array) when scanning a square region (typically 200 nm by 200 nm). These results were comparable to those obtained when the tip was not scanning (zero scan size). During the collection of a current−voltage curve, the instrument stopped lateral tip scanning and turned off the feedback. The sweep time for each curve was 150 μs, and the bias limits were −2 to +2 V. Each data set was subjected to a screening process where saturated responses were removed as described previously.[4] The peak currents and valley currents were determined by analyzing the first derivative of each I−V curve. These values were used to calculate a peak-to-valley ratio (PVR) for each peak. The large number of samples per scanning area (1024 per 0.04 μm^2 area (200 nm × 200 nm)) permitted the collection of a large number of data for each sample.

Current−Distance Spectroscopy. Current−distance (I−s) spectroscopy data were also collected on at least three samples with three different tips for each type of sample (C_{12}S-SAM, FcC_{11}S-SAM, β-CD-FcC_{11}S-SAM, and α-CD-FcC_{11}S-SAM). The tip was placed at various positions on the substrate, and the current was recorded as the tip was

retracted 2 Å. At least 50 curves were collected for each individual sample. Each curve was acquired at a set point of 10 pA and 1 V, and 32 points per curve were taken with an acquisition time of 100 μs.

Polarization Modulation Infrared Reflection Absorption Spectroscopy (PM-IRRAS). The PM-IRRAS spectra were recorded on a Digilab FTS 6000 spectrometer equipped with a step scan interferometer, liquid nitrogen cooled narrow band MCT detector, globar source, and a UDR-4 filter. The IR radiation was typically phase modulated at frequencies of 400 or 800 Hz at an amplitude of 1.0 or 2.0 λ HeNe while stepping at 0.5−2.5 Hz. A gold grid polarizer was used to obtain either s- or p-polarized radiation, which was then modulated by a Hinds ZnSe PEM operating at 37 kHz and amplitude of 0.5 λ (strain axis 45° to the polarizer) before reflecting off the sample at an incident angle of 80° from the surface normal. The spectra were recorded at room temperature at a resolution of 4 cm^{-1} and were the results of one scan with a spectral range of 900−4000 cm^{-1}. The digital signal processing (DSP) algorithm incorporated into the Digilab spectrometer software was used to obtain the spectra, which eliminates the need for a separate reference gold slide.

Acknowledgment. We thank Russell Miller for providing 11-ferrocenylundecanethiol, Scott Brewer and Angela Allen for assistance in collecting PM-IRRAS data, and the Office of Naval Research for funding under grant N00014-00-1-0633.

JA037651Q